RZ 3934 (# ZUR1806-032) 06/12/2018
Materials Science 4 pages

Research Report

Monolithic Integration of III-V on Si Applied to Lasing Micro-Cavities: Insights from STEM and EDX

M. Sousa, S. Mauthe, B. Mayer[1], S Wirths[2], H. Schmid, K.E. Moselund

IBM Research – Zurich
8803 Rüschlikon
Switzerland

[1]Now with MPI Munich, Germany

[2]Now with ABB Corporate Research, Baden, Switzerland

The final version of this manuscript has been published in:
M. Sousa, S. Mauthe, B. Mayer, S. Wirths, H. Schmid, K. E. Moselund
"Monolithic Integration of III-V on Si Applied to Lasing Micro-Cavities: Insights from STEM and EDX"
2018 IEEE 18th International Conference on Nanotechnology (IEEE-NANO), Cork, Ireland, 2018, pp. 1-4, doi: 10.1109/NANO.2018.8626223

Monolithic integration of III-V on Si applied to lasing micro-cavities: insights from STEM and EDX

M. Sousa, S. Mauthe, B. Mayer*, S Wirths*, H. Schmid, K.E. Moselund
IBM Research Zurich, Rueschlikon, Switzerland, email: sou@zurich.ibm.com

Abstract— Due to their high mobility and direct band gap, III-V materials promise good prospects of obtaining novel, high-performance devices for electronic and photonic applications. In this paper, two variants of the established Template Assisted Selective Epitaxy (TASE) technique [2-4] are explored to study the structural quality of GaAs and InGaAs microcavities monolithically integrated on Si (001). The first variant involves a one-step direct cavity growth (DCG), while the second relies on a two-step virtual substrate (VS) growth approach. The cavities obtained were investigated by Scanning Transmission Electron Microscopy (STEM) and Energy Dispersive X-Ray Spectroscopy (EDX); the findings have been correlated with the photoluminescence properties of the cavities. Both approaches enable monolithic integration of GaAs crystalline material in predefined oxide microcavities. In some cases, they allow the III-V materials to be grown as a single gain and do not lead to noticeable structural defects. InGaAs disks and ring cavities grown using the VS approach have also been investigated. Despite the presence of planar defects and rough surfaces, lasing could be achieved at low temperature.

I. Introduction

It is expected that more than billion computerized devices will be connected by 2020, such that the yearly global internet traffic will break the zettabyte ceiling [1]. Consequently, power consumption of integrated circuits will increase and a variety of devices will have to be integrated on same Si platforms. For integrated photonics in the Datacom industry, promising devices are lasers operating at wavelengths above 1.1 µm, where Si is transparent. To achieve integration densities comparable to that of electronics, the gain material must be grown (or bonded) on top of a Si substrate with high crystalline quality over a relatively large (~ 1 µm) and thick area (~ 100s of nm) by electronic standards.

The direct growth on Si is particularly challenging for III-V semiconductors, due to the large lattice mismatch and different thermal expansion coefficients involved. As an attempt toward the integration of III-V materials in actual devices, two variants of the TASE approach are investigated here, which allow III-V materials to be monolithically integrated on Si platforms. The first variant involves a direct (one-step) cavity growth (hereafter DCG, see Fig. 1a) [5], while the second relies on a two-step growth, here referred to as a virtual substrate growth (VS) approach [5-6], see Fig. 1b.

Integrating high-quality crystalline III-V layers using Metal Organic Chemical Vapor Deposition (MOCVD) on amorphous buried oxides can be quite challenging, it being noted that the oxide must be sufficiently thick to provide a satisfactory mode confinement.

Finally, outcomes of the structural investigations are correlated with the optical emission properties of the cavities. Results obtained for GaAs (disks) as well as InGaAs (disks and rings) lasing cavities are discussed.

II. Samples Preparation and Characterisation Techniques

A. Growth

In both the DCG and VS approaches, the III-V growth is performed by MOCVD, chosen here for its high selectivity of the deposition and the long diffusion length of the precursors. For GaAs, trimethylgallium (TMGa) and tertiary-butylarsine (TBAs) precursors are used, with a V-III ratio of 30 and a growth temperature of 600 °C.

For InGaAs, a trimethylindium (TMIn) precursor was added to the TMGa and TBAs; an In content of 30 % was targeted. The deposition was carried out at 560 °C, using a V-III ratio of 32.

The DCG process is summarized in Fig. 1a and otherwise described elsewhere in detail [5]. In a few words, a small opening (< 100 nm in diameter) is defined by dry reactive ion etching in an oxidized Si (001) substrate prior to depositing and patterning a sacrificial amorphous Si layer. After depositing an oxide shell by plasma enhanced chemical vapor deposition (PECVD), template openings are dry-etched and the sacrificial layer is selectively removed with XeF_2. Finally, the predefined small opening to the Si substrate allows for a single nucleation of the III-V at the Si and hence prevents the formation of antiphase defects and threading dislocations at the Si/III-V interface. The size and shape of the openings ensure precursors supply during the growth and, in addition, mechanically stabilizes the hollow template. The size of the optical cavity is determined by the growth duration. The results discussed in the following were obtained for 350 nm thick microdisks having diameters of ~ 1 µm.

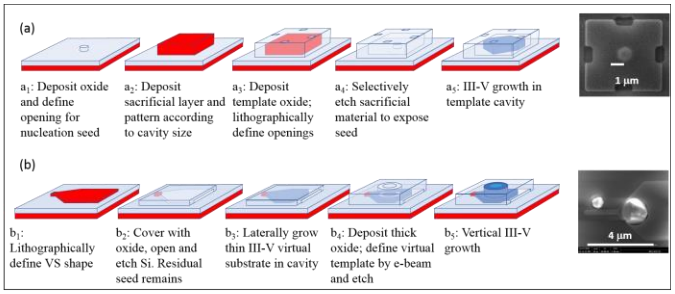

Fig.1: Schematics and SEM images (top views) of the two templates techniques: (a), direct cavity growth (DCG) and (b), virtual substrate growth (VS).

The VS approach (Fig 1b) relies on an SOI wafer, as explained in detail in [6,7]. Briefly, the top 50 nm (thick) Si is first patterned using e-beam lithography. Next, an oxide shell is deposited and partially etched with hydrofluoric acid (HF) on one side, to further expose Si and create a single point nucleation seed. The subsequent III-V lateral growth results in the desired virtual substrate. The growth is followed by a deposition of ~ 500 nm PECVD- SiO_2, which is then partially etched to act as a confined vertical cavity. Next, this cavity is filled with the III-V material during a second MOCVD-growth step, using the same growth parameters. The growth duration determines the thickness of the III-V material, while the lithographic step governs the cavity size and geometry. Only disk cavities have been investigated for GaAs while both disk and ring cavities were characterized for InGaAs. The disks are roughly 500 nm thick and 2 µm large. Geometrically, the rings were designed to be identical to the disks, except they include a 1 µm diameter disk opening in the center, where the opening is filled with SiO_2.

B. *Characterization Techniques*

To assess and optimize the III-V crystalline quality, cross-section lamellae of the obtained cavities were prepared using a FEI - Helios NanoLab 450S focused ion beam (FIB). The lamellas were first cut with an acceleration voltage of 30 kV. Then, final polishing steps have been performed at 5 kV to prevent as much as possible material degradation and changes of the structural properties. We further used a double spherical aberration corrected JEOL-ARM 200F Analytical High-Resolution Microscope, operated at 200 kV and equipped with a JEOL Dry SD100GV silicon drift detector with 100 mm^2 detection area for energy dispersive X-Ray spectroscopy (EDX) analyses, in order to image the III-V microstructure and map the various elemental species. Bright field (BF) STEM images are presented herein, which were acquired for a convergence semiangle of 25 mrad.

In addition, the Digital Micrograph software from Gatan Inc. was used for elemental map analyses. The In quantification of the InGaAs cavities was evaluated considering a Kramers background correction mode as well as a mixed k-factor for the quantification with a Casnati cross section model. The lamella thickness was assumed to be equal to 100 nm along the entire lamella. As a result of this approximation, the In contents discussed below should be considered qualitatively rather than quantitatively.

Prior to preparing the lamella, the samples were optically characterized using a micro-photoluminescence setup that consists of a pulsed supercontinuum laser, a cryostat, a spectrometer and an InGaAs photodetector [7]. Photoluminescence spectra and Input-Output light characteristics were obtained for temperatures ranging from 4 K to 300 K with a pulsed supercontinuum laser at 780 nm (78 MHz).

III. Experimental Results

A. *Direct Cavity Growth*

The DCG approach (Fig. 1a) led to three kinds of structures as depicted in Fig. 2a-c. In some cases (as in Fig. 2a), the initial nucleation did not take place at the bottom of the cavity, but most likely near an impurity. This led to a cavity filled with polycrystalline GaAs, loaded with dislocations, and exhibiting a rough top surface. In other cases (Fig. 2b), the nucleation took place at the silicon surface and the lateral cavity was satisfactorily filled. Still, lattice defects such as stair-rod dislocations happened to grow from the seed and propagate up to the top surface of the cavity, resulting in multiple grains with different orientations and non-parallel facets. Such devices were unsurprisingly not able to lase, owing to the multiple interfaces formed, which prevent optimal light confinement in the cavity.

In more favorable cases (Fig. 2c.), however, BF STEM images indicate that the crystalline defects remain confined within the seed. In such cases, a single GaAs grain without any structural defect could be achieved, yielding a micro cavity that lases at room temperature. Still, a closer look at the GaAs, using a fast Fourier transform of a high-resolution image (such as shown in Fig.1d) revealed that the GaAs grain was tilted (~ 8°) compared to the Si seed and oriented along the [11–2] direction (probably due to an overetching of Si). Interestingly, this approach allows a smooth top surface to be systematically achieved, as the top surface quality is governed by the cavity. EDX measurements did not show any elemental diffusion from SiO_2 into GaAs. According to the optical measurements, a lasing threshold of 2.5 pJ/pulse at room temperature could be achieved [5].

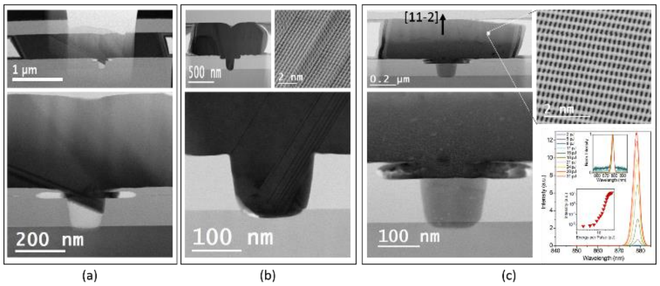

Fig.2: Bright Field STEM images of three GaAs microcavities grown according to the Direct Cavity Growth approach. (a), (b): non-lasing cavities overview and zoom over the seed region. Inset in (b): zoom over a stair-rod dislocation defect observed in the GaAs seed. (c): defect-free cavity showing lasing up to room temperature [5].

B. *Virtual Substrate Growth*

1) GaAs

Using the VS approach on GaAs, two kinds of disk cavities could be observed (Fig. 3a,b). The first VS growth run resulted in VS cavities that were only partially filled (Fig. 3a). Such cavities exhibited a rough top surface, most likely due to a mismatch between the expansion of the VS film and the position of the second vertical template mask. In addition, an overetching of the virtual substrate region was observed. Such defective structures were accordingly not able to lase.

However, subsequent runs yielded microdisks with flat top surfaces (Fig. 3b), consisting of single-grain GaAs oriented along the [–110] direction, which did lase up to 250 K (Fig. 3c, 3d).

The devices obtained with the VS approach do not necessarily exhibit a smooth top surface as the surface quality is now governed by the III-V growth along the virtual substrate path. This is expected to impact the quality factor of the cavity and thus the lasing performance. A more detailed analysis of the lasing properties is given elsewhere [6].

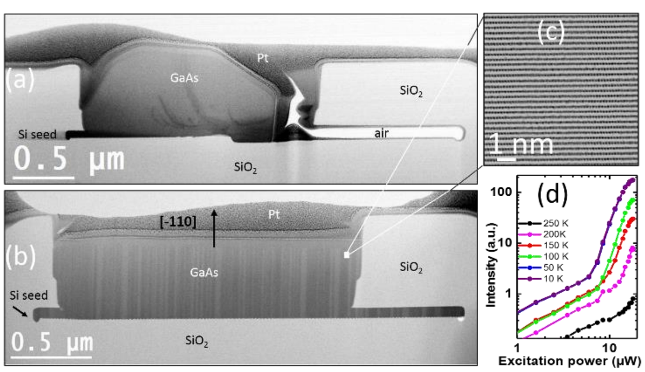

Fig.3: Bright Field STEM images of two GaAs cavities grown with the VS growth approach. (a): non-lasing cavities overview (b), (c): defect-free cavity, (d): Input-output light characteristic for temperatures up to 250 K (d) [6].

2) InGaAs

Finally, InGaAs microcavities with two different geometries, namely a disk and a ring, have been grown and characterized.

BF STEM images clearly show that the cavities are now polycrystalline and present rough top surfaces (Fig. 3a and Fig. 4a) and, this, for both geometries. Moreover, the atomic resolution BF STEM images have revealed a change in the orientation of the InGaAs dumbbells due to planar defects (Fig. 4c, 5c). Indeed, stacking faults and twin boundaries were clearly observed for the disk and ring geometry, respectively.

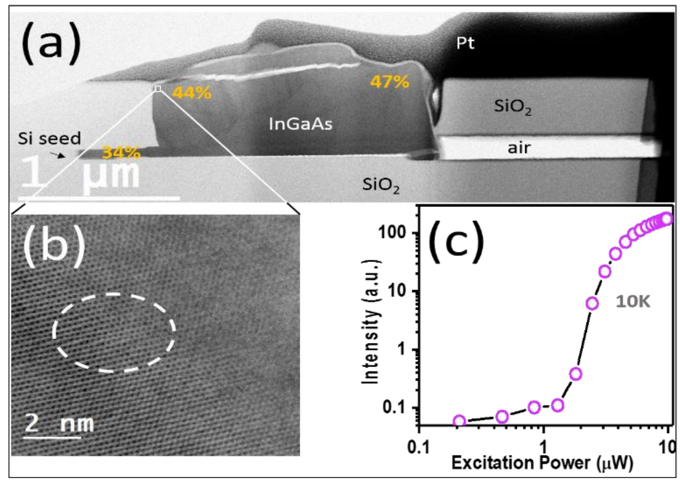

Fig.4: (a) Bright Field STEM images of the InGaAs microcavity and In content evaluated from EDX maps. (b) is a zoomed image over a grain boundary and a stacking fault while (c) depicts a corresponding input-output light characteristic measured at 10 K [7].

EDX analyses were carried out for each of the two geometric structures. For the disk, an indium concentration gradient ranging from 34 % (at the bottom) to 47 % (at the top) was observed (Fig. 3b). Comparable results were obtained for the Indium concentration in the ring cavity, it being reminded that the latter was processed in much the same way as the disk. Namely, an In content of 22 % was seen close to the seed, vs. 41 % near the top right. Again, the resulting values are qualitative only, owing to approximations made during the calculations: we evaluate the simulation error to be on the order of ± 3 %. Still, the results obtained are sufficient to ascertain the existence of a gradient of In concentration, which could be a consequence of the different diffusions of precursors as occurring during the virtual substrate and cavity filling. Indeed, two mechanisms may be involved in the transport of In and Ga precursors during the MOCVD growth: the diffusion in vapor and the surface diffusion [8].

For the ring geometry, EDX further revealed a ~ 25 nm (In, Ga, As, Si and O) intermixing area at the InGaAs/SiO_2 inner interface. An optimization of this interface should result in enhancing the lasing effect.

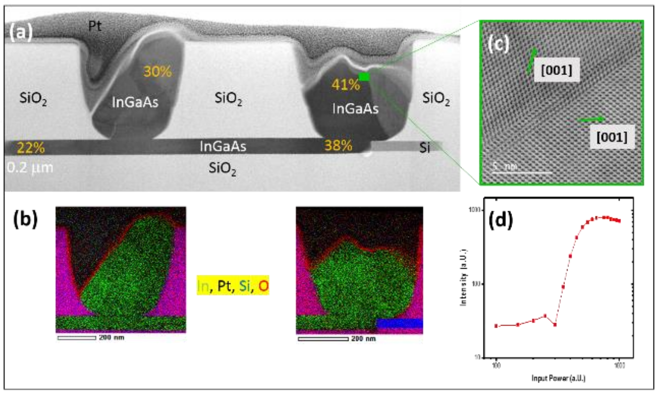

Fig 5: (a) BF STEM cross section; (b): EDX overview map; (c) high resolution image over a twin boundary; (d) corresponding input-output light characteristic measured at 6.3 K [7]

Despite a rough top surface (Fig. 4a, 5a), grains tilting and other defects (Fig. 4c, 5c), lasing could be achieved up to 200 K for the ring and the disk geometry, with respective lasing threshold of 9.5 pJ/ pulse and 6.8 pJ/pulse measured at 10 K (Fig. 4d, 5d) [7].

IV. CONCLUSION

Lasing III-V microcavities were grown on Si using two variants of TASE. Both made it possible to obtain (i) micrometer square cavities of high crystalline quality (yet with a higher success rate for the VS variant); and (ii) a large single GaAs grain with a smooth top surface, lasing at room temperature. Applying the VS approach to InGaAs, rough and polycrystalline InGaAs microcavities could be obtained. The two geometries investigated have led to the same conclusion: the InGaAs devices obtained are polycrystalline, while it is not possible to achieve a constant In concentration throughout the cavity. However, lasing was observed for temperature up to 200 K, together with low temperature (10 K) lasing thresholds, i.e., of 9.5 pJ/ pulse for the disk and 6.8 pJ/pulse for the ring structures. This result is promising; improved control over the III-V elemental species diffusion as well as interfaces with SiO_2 shall manifestly allow the performances of such devices to be improved.

ACKNOWLEDGMENT

The authors gratefully acknowledge the support of L. Czornomaz, S. Reidt and M.D. Rossell (EMPA, Switzerland). Also acknowledged is the financial support from the EU H2020 MODES (704045) project as well as the ERC project PLASMIC (678567).

*B. Mayer and S. Wirths are currently at MPI Munich, Germany and ABB Corporate Research, Baden Switzerland, respectively.

REFERENCES

[1] https://www.ncta.com/platform/industry-news/infographic-the-growth-of-the-internet-of-things/

[2] Schmid, H.; Borg, M.; Moselund, K.; Gignac, L.; Breslin, C. M.; Bruley, J.; Cutaia, D.; Riel, H. Template-Assisted Selective Epitaxy of III-V Nanoscale Devices for Co-Planar Heterogeneous Integration with Si. *Appl. Phys. Lett.* **2015**, *106* (23), 233101.

[3] Schmid, H.; Cutaia, D.; Gooth, J.; Wirths, S.; Bologna, N.; Moselund, K. E.; Riel, H. Monolithic Integration of Multiple III-V Semiconductors on Si for MOSFETs and TFETs. *2016 IEEE International Electron Devices Meeting (IEDM)*; IEEE, 2016; p 3.6.1-3.6.4.

[4] Czornomaz, L.; Uccelli, E.; Sousa, M.; Deshpande, V.; Djara, V.; Caimi, D.; Rossell, M. D.; Erni, R.; Fompeyrine, J. "Confined Epitaxial Lateral Overgrowth (CELO)". *2015 Symposium on VLSI Technology (VLSI Technology)*; IEEE, 2015; pp T172–T173.

[5] Wirths, S.; Mayer, B.; Schmid H.; Sousa, M.; Gooth, J.; Riel, H.; Moselund, K. "Room Temperature Lasing from Monolithically Integrated GaAs Microdisks on Si", ACS Nano 12, 3, 2169-2175

[6] B. Mayer, to be published.

[7] S. Mauthe, B. Mayer, M. Sousa, G. Villares, P. Staudinger, H. Schmid, K.E. Moselund, "Monolithically integrated InGaAs microdisk lasers on silicon using template-assisted selective epitaxy," *Proc. SPIE 10672, Nanophotonics VII, 106722U (May 2018).*

[8] Borg, M., Schmid, H., Moselund, K. E., Cutaia, D., and Riel, H., "Mechanisms of template-assisted selective epitaxy of InAs nanowires on Si," Journal of Applied Physics 117(14) (2015).